

# Detection of lot-to-lot variations in the amorphous microstructure of lyophilized protein formulations

Yutaka Hirakura<sup>\*</sup>, Hideto Yamaguchi, Masayasu Mizuno, Hideo Miyanishi, Satoshi Ueda, Satoshi Kitamura

*Pharmaceutical Analysis, Pharmaceutical Research and Technology Laboratories, Astellas Pharma Inc., 180 Ozumi, Yaizu, Shizuoka 425-0072, Japan*

Received 6 September 2006; received in revised form 13 February 2007; accepted 12 March 2007

Available online 14 March 2007

## Abstract

Reconstitution of lyophilized protein formulations sometimes results in a cloudy solution, depending on the compositions and manufacturing conditions, which causes quality concerns. In this study, the lyophilized protein formulation of recombinant human Interleukin-11 (rhIL-11) was investigated using different lots with varying dissolution behaviors upon reconstitution due to differing processing conditions. In an attempt to distinguish the solid structures in the different lots, relatively new techniques such as inverse gas chromatography (IGC) and thermally stimulated depolarized current (TSDC) as well as powder X-ray diffraction (PXRD) and differential scanning calorimetry (DSC) were adopted for analysis. PXRD, DSC, and IGC all failed to distinguish between the solid structures, but TSDC was able to discern the differences. Interestingly, TSDC suggested that the variations in dissolution behavior were attributable to the differences in molecular mobility and the micro heterogeneity of amorphous components in the solid structures. Since even the cloudiest reconstituted solutions became transparent in several minutes, it was likely that the differences in the solid structures of the different lots of lyophilized cakes were slight. This study demonstrates the usefulness of TSDC in the analysis of lot-to-lot variations in amorphous pharmaceuticals.

© 2007 Elsevier B.V. All rights reserved.

**Keywords:** Lot-to-lot variation; TSDC; TSC; Amorphous; Heterogeneity; Lyophilized formulation

## 1. Introduction

Lyophilized protein formulations sometimes cause dissolution problems upon reconstitution due to differences in composition, the manufacturing process, and storage conditions. There are many studies on lyophilized protein formulations in the literature that report on how to control product temperature during manufacturing, how to choose appropriate stabilizing excipients, and how to stabilize products during both manufacturing and storage from a mechanistic point of view (Carpenter et al., 1997; Tang and Pikal, 2004). In these studies, a variety of analytical tools are used to examine the manufacturing processes and to characterize the physicochemical properties of the freeze-concentrate as well as the solid structure of the lyophilized cake (Nail et al., 2002). It is, however, often difficult to obtain consistent quality from lot-to-lot because freeze-drying is a complex

mixture of dynamic and non-equilibrium processes, which may cause a diverse variety of amorphous forms and heterogeneity to occur in the lyophilized cake (Hancock et al., 2002). Since it is essential to secure lot-to-lot consistency in pharmaceutical production, it is worthwhile to search for new techniques capable of sensitively discerning variations in product quality.

Inverse gas chromatography (IGC) is a method of chromatographic analysis used to detect the surface free energy and acid–base (acceptor–donor) properties of solid materials. Unlike in ordinary gas chromatography, the solid sample is packed in a column as the stationary phase, and then vaporized organic solvents are introduced into the column to probe the solid surface (Grimsey et al., 2002). There has already been extensive work done on developing applications for the pharmaceutical research field, including the examination of batch-to-batch variation (Ticehurst et al., 1994, 1996), changes in the surface energetics that occur with milling (Roberts et al., 1994; York et al., 1998; Feeley et al., 1998), the effect of humidity on surface energetics (Djordjevic et al., 1992; Sunkersett

<sup>\*</sup> Corresponding author. Tel.: +81 54 627 7294; fax: +81 54 629 6455.  
E-mail address: [yutaka.hirakura@jp.astellas.com](mailto:yutaka.hirakura@jp.astellas.com) (Y. Hirakura).

et al., 2001), changes in surface properties caused by granulation (Yokoi et al., 2004), determination of the glass transition temperature (Surana et al., 2003), and prediction of the quality of powder for inhalation (Cline and Dalby, 2002; Tong et al., 2006). With IGC, unlike conventional methods such as water penetration, the highest energy sites on the surface are probed more readily than the lower ones because probe molecules are flown at infinite dilution (Newell and Buckton, 2004). This infers that IGC is a very sensitive tool capable of detecting slight differences between solid surfaces. In fact, Ticehurst et al. (1994) demonstrated that IGC was able to discern variations between batches of salbutamol sulfate that were not distinguishable when FT-Raman or X-ray diffraction were used. Ticehurst et al. (1996) also showed that IGC was capable of discerning batch-to-batch variations in  $\alpha$ -lactose monohydrate that were not distinguishable when conventional analytical methods were used.

Thermally stimulated depolarized current (TSDC) is a method of thermal analysis used to detect dielectric relaxation. TSDC detects depolarized currents generated when polarized dipoles relax as the temperature increases (Shmeis et al., 2004a). This highly sensitive system is capable of detecting currents as small as a femto-ampere ( $10^{-15}$  A). Although it had been widely used to study the dynamics and molecular motions in polymer science (Zielinski and Kryszewski, 1977), TSDC was only recently introduced to the pharmaceutical research field. Shmeis et al. (2004a,b) compared TSDC with differential scanning calorimetry (DSC) and found that TSDC was able to detect phase transitions in amorphous solid dispersion that were not detectable using DSC. These transitions included  $\alpha$ -relaxation, where only a small heat capacity change occurred with strong glass. TSDC was also capable of detecting a  $\beta$ -relaxation event, which was totally undetectable using DSC, which demonstrates the excellent sensitivity of TSDC. Samouillan et al. (2002) examined the physicochemical properties of elastin and linked its relaxation behavior with its molecular architecture, which demonstrates the usefulness of TSDC in analyzing protein configurations. Proteins consist of polar repeating units in peptide bonds that are likely to be sensitive to dielectric polarization.

In this study, the solid structure of the lyophilized formulation of recombinant human Interleukin-11 (rhIL-11) was investigated. It was previously demonstrated that the dissolution behavior of the lyophilized formulation varied depending on the processing conditions (freezing conditions) (Hirakura et al., 2004). The temperature histories of the freezing phase had differential physicochemical impacts on the formulation, and their contribution to the occurrence of cloudiness upon reconstitution was investigated. Circumstantial evidence suggested that the variations in dissolution behavior associated with different processing conditions were a result of the differences in the disposition of the amorphous components such as the protein and dibasic phosphate anion in the lyophilized cake. It was suggested that the cationic protein ( $pI > 11.5$ ) was flanked by dibasic phosphate anions, which are divalent, through electrostatic attraction and only in a barely soluble lyophilized cake. In this study, IGC and TSDC were used to discern the differences in the lyophilized

cakes, and TSDC was found to be useful for this purpose. Powder X-ray diffraction (PXRD) and differential scanning calorimetry (DSC) were also used for reference. The literature search indicated that this is the first application of TSDC for the detection of lot-to-lot variations in the solid structure of lyophilized protein formulations.

## 2. Materials and methods

### 2.1. Materials

The organic solvents used for IGC and glycine used for PXRD were purchased from Kanto Chemical (Tokyo, Japan).

### 2.2. Freeze drying

Recombinant human Interleukin-11 (rhIL-11) solution was supplied by Wyeth Research. The solution was diluted and freeze-dried according previously reported procedures (Hirakura et al., 2004). The solution (5 mg/ml rhIL-11, 300 mM glycine, 10 mM sodium phosphate, pH 7.0) was filtered through a bottle-top filter equipped with a micro-porous membrane made from polyethersulfone (200 nm in pore size, Nalge Nunc Int., New York), manually dispensed into glass ampoules (1 ml each), and placed on a temperature-controlled shelf in a lyophilizer (R2L-100KPS, Kyowa Vacuum Engineering, Tokyo). After an ice nucleation procedure was begun in the lyophilizer at  $-6^{\circ}\text{C}$ , the ampoules were left at that temperature for 20 h, and then cooled below  $-25^{\circ}\text{C}$  (typically  $-28^{\circ}\text{C}$ ) (pretreated formulations). The door of the lyophilizer was then opened and another group of fresh ampoules was put on the cooled shelf ( $-28^{\circ}\text{C}$ ) (untreated formulations). These two groups of formulations were exposed to almost the same process except that the pretreated formulation had been exposed to the pretreatment storage phase. The cooling rates for both formulations during the freezing phase ( $-6^{\circ}\text{C}$  to lower than  $-25^{\circ}\text{C}$ ) were almost the same, ranging from around 1 to  $2^{\circ}\text{C}/\text{min}$ . The frozen samples were then vacuum-dried.

### 2.3. Turbidity measurement

The turbidity of a reconstituted solution was defined by optical density at 650 nm. Water for injection (1 ml) was applied to an ampoule to let the lyophilized cake disperse in the medium. After the cake was fully dispersed, the cloudy solution was transferred to a plastic cell. The cell was immediately mounted on the sample holder of a spectrophotometer (U-3300 spectrophotometer, Hitachi, Tokyo) for measurement.

### 2.4. Powder X-ray diffraction (PXRD)

An X-ray diffractometer (RINT-TTRIII, Rigaku Corporation, Tokyo) equipped with a Cu  $K\alpha$  source operating at a tube load of 50 kV and 300 mA was used. The divergence slit was 1 mm wide, and both the scattering slit and receiving slit were left open. Each sample was scanned between  $5^{\circ}$  and  $40^{\circ}$  ( $2\theta$  with

a step size of  $0.02^\circ$  and a scan rate of  $4^\circ/\text{min}$ ). The diffracted X-ray was detected using a scintillation counter. Pure  $\beta$ -glycine crystals were prepared by recrystallizing them according to the method reported by Drebuschak et al. (2002), with a minor modification. The glycine crystallinity in the lyophilized cakes was estimated by comparing the total peak intensities between the lyophilized cake and pure  $\beta$ -glycine. The peak intensities observed using lyophilized cakes were compensated for by the glycine fraction [approximately 78% (w/w)] in the solid samples.

## 2.5. Inverse gas chromatography (IGC)

A commercial inverse gas chromatograph was used for analysis (IGC system, Surface Measurement Systems, London, UK). The oven of a gas chromatograph (HP6890, Agilent Technologies, Santa Clara, CA) was used to maintain the probe gas temperature at  $30^\circ\text{C}$ . A silanized glass column (i.d., 3 mm; column length, 30 cm) was plugged with dimethyldichlorosilane silanized glass wool at one end, weighed, filled with solid sample, tapped for 10 min, again weighed, and plugged up with the same glass wool to fix the solid sample. The column was placed in the column oven and maintained at  $30^\circ\text{C}$ . Helium was used as the carrier gas (flow rate: 10 ml/min), and several kinds of probe gases (undecane, decane, nonane, octane, heptane, chloroform, acetone, ethyl acetate, and ethanol) were serially injected into the column. The column was equilibrated for 24 h at  $30^\circ\text{C}$  and 0%RH before measurement to completely dry the sample. Measurements were carried out at  $30^\circ\text{C}$  and 0%RH. A flame ionization detector (FID) was used to detect the probe molecules.

Data were analyzed according to Schultz and Lavielle (1989). The net retention volume ( $V_N$ ) is related to the dispersive component of the surface free energy of the solid ( $\gamma_s^d$ ) and probe ( $\gamma_L^d$ ) as follows,

$$RT \ln V_N = 2N_A(\gamma_s^d)^{1/2}a(\gamma_L^d)^{1/2} + C$$

where  $R$  is the gas constant,  $T$  the temperature,  $N_A$  the Avogadro's number,  $a$  the surface area of the adsorbed probe molecule, and  $C$  is a constant. When  $RT \ln V_N$  is plotted against  $a(\gamma_L^d)^{1/2}$ , alkanes yield a straight line, and the dispersive component of the surface free energy of the solid ( $\gamma_s^d$ ) is calculated using the slope of the alkane line [ $2N_A(\gamma_s^d)^{1/2}$ ]. The deviation from the alkane line along the Y-axis (when polar probes are used) represents the specific component of the surface free energy of the solid ( $\Delta G_A^{SP}$ ).  $\Delta G_A^{SP}$  can be reduced to the following equation according to Gutmann (1978) and Drago et al. (1971):

$$\Delta G_A^{SP} = K_A DN + K_D AN^*,$$

where DN is the donor or base number of the adsorbed probe molecule, and  $AN^*$  is the acceptor or acid number of the adsorbed probe molecule corrected to take dispersive contributions by Riddle and Fowkes into account (1989). By measuring the value of  $\Delta G_A^{SP}$  using several probe vapors and plotting

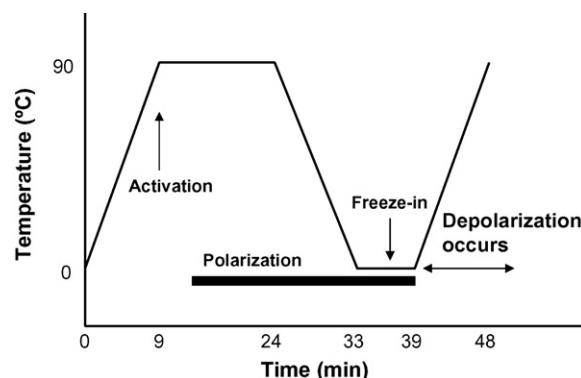


Fig. 1. A schematic view of the experimental program for TSDC is shown.

$\Delta G_A^{SP}/AN^*$  versus  $DN/AN^*$ , the values of  $K_A$  and  $K_D$  are calculated for the solid of interest.

## 2.6. Thermally stimulated depolarized current (TSDC)

A TSDC spectrometer (TS-POLAR, Rigaku Corporation, Tokyo, Japan) was used to measure dielectric relaxation as a function of temperature. After the lyophilized cake was removed from the ampoule and mixed well to achieve homogeneity, 15 mg of the powder was compressed at 400 N ( $4.0 \times 10^6$  Pa) for 1 min to form a tablet with an average thickness of 0.5 mm. The tablet was placed on the sample holder and fixed between the electrodes of a parallel plane capacitor. An insulator film was inserted between the tablet and one of the electrodes to cut out the direct current. The experimental program is illustrated in Fig. 1. The tablet was heated to  $90^\circ\text{C}$  at a rate of  $10^\circ\text{C}/\text{min}$  and held at the same temperature for 5 min. After an electric field of 50 V/mm was applied between the electrodes, the tablet was kept at  $90^\circ\text{C}$  for 10 min to cause static polarization of the dipoles to occur. The tablet was then cooled at a rate of  $10^\circ\text{C}/\text{min}$  and kept at  $0^\circ\text{C}$  for 6 min to freeze-in the polarization. After the electric field was removed, the tablet was heated at the same rate of  $10^\circ\text{C}/\text{min}$ . Relaxation of the oriented dipoles was measured as a function of temperature. Measurements were carried out in a dry helium atmosphere.

## 2.7. Differential scanning calorimetry (DSC)

A spatula was used to mix the lyophilized powder in an opened ampoule until uniformity was achieved. Sample was then taken out, placed in an aluminum pan, and set inside the furnace of a DSC measurement system (Q1000, TA instruments, New Castle, DE, USA) equipped with a refrigerated cooling system (RCS, TA instruments, New Castle, DE, USA). An aluminum pan was crimped for effective heat conduction, and an empty pan was used as a reference. Sample was heated to  $80^\circ\text{C}$  and held at the same temperature for 5 min. After it was cooled to  $-10^\circ\text{C}$ , the sample was heated to  $150^\circ\text{C}$  at a rate of  $20^\circ\text{C}/\text{min}$ . Measurements were made under a constant flow of nitrogen ( $50 \text{ ml}/\text{min}$ ).

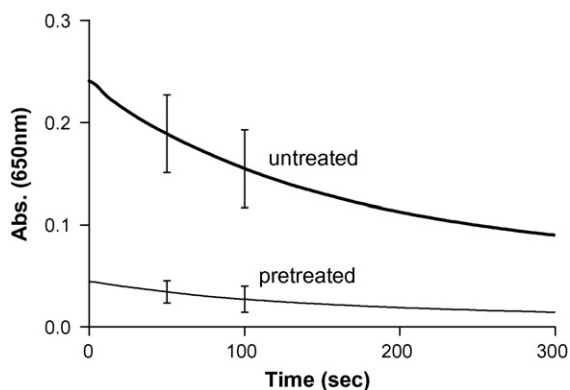


Fig. 2. Dissolution properties of rhIL-11 lyophilized formulations are shown. The absorbance at 650 nm of reconstituted solutions is shown as a function of time. Commercial water for injection (WFI) was applied to an ampoule. Symbols: untreated formulation (bold), pretreated formulation (thin). The error bars represent standard deviations ( $n = 3$ ). This figure was reprinted from Fig. 1 of a paper previously published in this journal (Hirakura et al. (2004) 53–67) after modification.

### 3. Results and discussion

#### 3.1. Measurement of absorbance at 650 nm

In order to illustrate the contrast in dissolution properties of the lyophilized cakes, absorbance over time at 650 nm is shown for rhIL-11 reconstituted solutions that were created using a batch of commercial water for injection (WFI) (Fig. 2). A lyophilized cake produced using the standard temperature program (untreated formulation) formed a cloudy solution upon reconstitution (bold line). The cloudiness of the solution, however, is not of permanent nature, and the solution became kinetically less cloudy with time and almost transparent in 20–30 min at the most. In contrast, a lyophilized cake produced by the pretreatment method (pretreated formulation) promptly dissolved in WFI (thin line). It should be noted that no differences were observed between untreated and pretreated formulations after the reconstituted solutions became transparent. Clearly, these results suggest that there are originally some differences in the solid structures between untreated and pretreated formulations although they have the same chemical compositions and there are no differences in the reconstituted solutions once these components are dissolved. The cloudiness never occurred with protein-free formulations irrespective of the processing conditions, indicating that the protein is necessary for the occurrence of cloudiness (not shown).

#### 3.2. Powder X-ray diffraction (PXRD)

The first method employed to examine the predicted differences in the solid structure was powder X-ray diffraction. Fig. 3 demonstrates the PXRD patterns obtained using the untreated and pretreated formulations. It is clear that there were no differences between these diffraction patterns, which typically represent the glycine  $\beta$ -form. The total integrated intensities of the diffraction peaks observed between  $5^\circ$  and  $40^\circ$  were  $1.40 \pm 0.11 (\times 10^6)$  and  $1.33 \pm 0.10 (\times 10^6)$  for the untreated

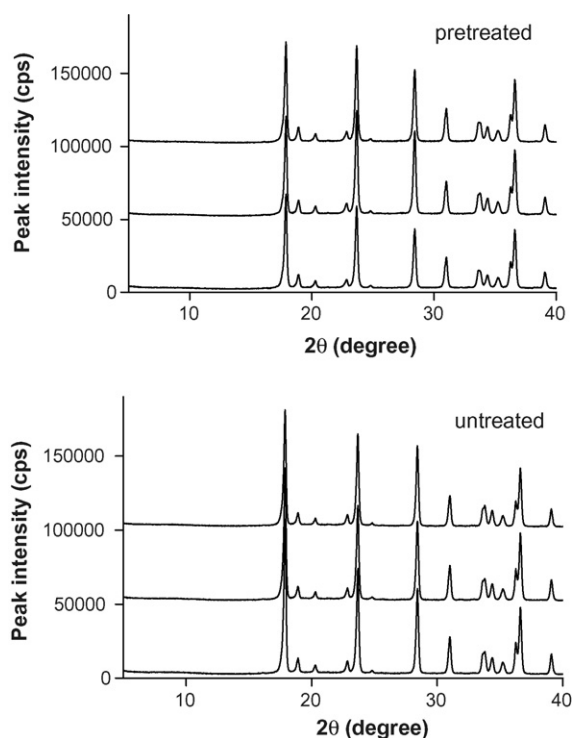


Fig. 3. The powder X-ray diffraction (PXRD) patterns of the untreated and pretreated formulations are shown. Pretreated formulation (upper), untreated formulation (lower). Note that the three traces for each formulation were obtained using lyophilized cakes from different ampoules.

and pretreated formulations, respectively ( $n = 3$ ). These results indicate that the glycine polymorphism, crystal habit, and crystallinity are the same in both formulations. When compared with the PXRD pattern of the pure glycine  $\beta$ -form, the glycine was estimated to be approximately 90% crystalline ( $91.4 \pm 6.8\%$ ,  $n = 3$ ), which in turn indicates that the remaining 10% glycine was amorphous in both formulations. No traces representing crystals of sodium phosphate or protein were found in the diffraction patterns, indicating that these components are amorphous. These results suggest that the predicted structural differences between the formulations are not due to glycine polymorphism, crystal habit, or crystallinity, but to the variations in the amorphous structures.

#### 3.3. Inverse gas chromatography (IGC)

IGC was then adopted for analysis. IGC gives information on the physical properties of surfaces, such as wettability and polarity, that can be crucial in the dissolution of solid pharmaceuticals. Table 1 summarizes the IGC results obtained using untreated and pretreated formulations. Apparently, there are no significant differences between the surface properties of the untreated and pretreated formulations. No significant differences in the dispersive component of the surface free energy ( $\gamma_s^d$ ) could be observed between the untreated and pretreated formulations. No significant differences in the change in free energy upon adsorption ( $\Delta G_A^{SP}$ ) because of specific interactions with the polar probe molecules could be observed between the untreated and pretreated formulations. However, the change in free energy upon

Table 1  
IGC data obtained using untreated and pretreated formulations

Lot	$\gamma_s^d$ (mJ/m <sup>2</sup> )	$\Delta G_A^{SP}$ (kJ/mol)				$K_A$	$K_D$
		Chloroform	Acetone	Ethylacetate	Ethanol		
Untreated	59.84 (2.40)	1.98 (0.23)	9.20 (0.39)	11.25 (0.26)	16.56 (0.36)	0.14 (0.00)	0.06 (0.01)
Pretreated	58.04 (1.75)	1.94 (0.10)	9.11 (0.32)	11.44 (0.53)	16.47 (0.43)	0.14 (0.01)	0.06 (0.00)

The values in parentheses are standard deviations ( $n=3$ ).

adsorption ( $\Delta G_A^{SP}$ ) is much larger with basic probe molecules, which indicates that the lyophilized cakes have more surface area of an electrophilic nature. These results suggest that the predicted structural differences between the formulations are not due to the surface properties but to the internal (core) structures of the lyophilized cakes.

### 3.4. Thermally stimulated depolarized current (TSDC)

TSDC was found to be useful in detecting the structural differences between the lyophilized cakes. Fig. 4 shows the depolarization currents observed using untreated and pretreated formulations. Two distinct but broad depolarization peaks were observed for both formulations. Obviously, these peaks shifted to higher temperatures in the untreated formulations. The traces measured using samples from different ampoules were reproducible, which indicated that these traces are distinct representations of the microstructures of the formulations. Since there were no differences in glycine polymorphism, crystal habit, or crystallinity (Fig. 3), the differences in the traces observed between the two formulations were due to those of the amorphous structures. The range of temperatures over which depolarization currents occur are representative of the distribution of the solid structure relaxation times (Van Turnhout, 1998). Moura Ramos et al. (2005) stated that amorphous substances generally exhibit broader and stronger peaks than crystalline ones. While crystalline substances consist of ordered structures with specific relaxation times, amorphous ones include heterogeneous structures whose relaxation times are spread out over

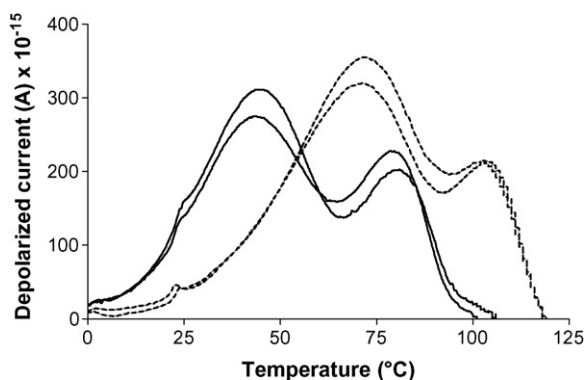


Fig. 4. Thermally stimulated depolarized current (TSDC) traces observed using different lots of the lyophilized formulations are shown. The vertical and horizontal axes denote a depolarization current in femto-amperes and temperature, respectively. Symbols: pretreated (continuous); untreated (dotted). Note that the two traces for each formulation were obtained using lyophilized cakes from different ampoules.

a wide temperature range (Moura Ramos et al., 2005). Therefore, it is natural that the broad depolarization peaks observed in Fig. 4 originate largely from the amorphous components. It is most likely that the differences in microstructure represented by the depolarization currents reflect the differences in the physicochemical conditions of the amorphous components.

It should be mentioned that reduced molecular mobility was noted in the untreated formulation. This was apparent because of the rightward shift of the depolarization peaks, which is indicative of slower dipole relaxation times. Ikeda et al. (2005) demonstrated that, in the TSDC spectra of terfenadine polymorphs, the peak approximate temperatures were 125 °C for form I, 95 and 120 °C for form II, and 65 and 80 °C for the amorphous form. Terfenadine is a monotropic anti-histamine drug, and form I is more stable than form II and the amorphous form (Yoshihashi et al., 2000). These indicate that rightward peak shifts represent the stable forms of the drug and reduced molecular mobility, hence slower dipole relaxation times.

### 3.5. Differential scanning calorimetry (DSC)

Fig. 5 shows DSC traces obtained using pretreated and untreated formulations. To compare them with the TSDC results, the sample settings and experimental protocols used were similar to those for TSDC. There appeared to be no characteristic differences between the two formulations, which were scarcely discernible using this analytical method. A closer look at the figures might reveal that the small heat capacity increases (downward baseline shifts) observed between 80 and 120 °C were glass

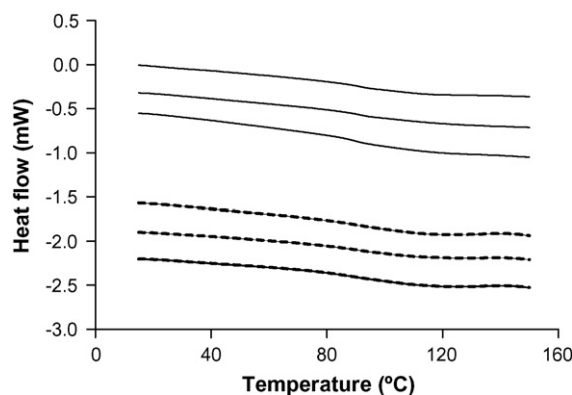


Fig. 5. Differential scanning calorimetry (DSC) traces observed using different lots of the lyophilized formulations are shown. The vertical and horizontal axes denote heat flow and temperature, respectively. Symbols: pretreated (continuous); untreated (dotted). Note that the three traces for each formulation were obtained using lyophilized cakes from different ampoules.

transitions and that the glass transition temperatures ( $T_g$ ) had shifted to slightly higher temperatures with the untreated formulation (dotted lines). However, even if the downward shift is caused by glass transition, such a subtle change in the trace does not help distinguish between the untreated and pretreated formulations from a practical point of view. These results indicate that TSDC is capable of distinctly characterizing slight differences in the solid structure that DSC can barely distinguish, which highlights the excellent sensitivity of TSDC as an analytical tool.

### 3.6. Distinction of small differences in the amorphous microstructure using TSDC

It is likely that the differences in the solid structure occurring between the untreated and pretreated formulations are slight because, unlike other cases where solutions remain cloudy after reconstitution, the cloudiness observed with the untreated formulation disappeared in minutes (Fig. 2). This is also supported by the fact that PXRD and DSC could not discern the differences between the solid structures. Interestingly, the variations in the lyophilized cakes could not be discerned using IGC (Table 1), which measures the surface free energy of solid materials. The failure of discrimination suggests that the slight differences between the formulations are related to the internal core structures. This observation coincides with the fact that dissolution involves several complex processes that may include not only wettability, but also disintegration and solubility (Backton, 1995). Disintegration and dissolution are due not only to the surface properties but also to the interior structures of solids. This is particularly true for the dissolution of a drug product which involves the integrated mixture of many ingredients.

The protein and dibasic phosphate anion are most probably the amorphous components that respond differently to the electric field in the TSDC experiments (Fig. 4). There were no differences in glycine polymorphism, crystal habit, or crystallinity between the formulations, and sodium phosphate and the protein were found to be amorphous in both formulations (Fig. 3).  $^{31}\text{P}$ -solid state NMR analysis (not shown) confirmed that sodium phosphate is indeed amorphous in the lyophilized cakes. It should be noted that, for a pretreated formulation, sodium dibasic phosphate became crystallized as dodecahydrate during freezing and phase-separated from the protein, whereas, in an untreated formulation, the buffer salt stayed amorphous and dibasic phosphate anions were flanked by the protein all through the processes (Hirakura et al., 2004). In the pretreated formulation, sodium dibasic phosphate dodecahydrate crystals which crystallized during freezing later dehydrated and disintegrated into amorphous form during drying (Hirakura et al., 2004). In general, sodium dibasic phosphate can crystallize out of the solution (phase-separate) during freezing, leaving only monobasic salt in the freeze-concentrate (Randolph, 1997). It is also known that sodium dibasic phosphate crystallizes into dodecahydrate during freezing (Murase and Franks, 1989; Gomez et al., 2001) and returns to amorphous form during drying (Pyne et al., 2003a,b). Our previous observations were consistent with the other studies and led to the conclusion that the major dif-

ferences in the solid structures of the untreated and pretreated formulations are in the disposition of the amorphous components such as the protein and dibasic phosphate anions. In addition, no evidence or rationale has been presented that would suggest that there are large enough differences in the physicochemical condition of amorphous glycine to generate different responses to the electric field.

Many energetically indistinct gradated states can exist in a glassy microstructure, depending on the processing conditions, because glassy systems stay in non-equilibrium by nature (Hancock et al., 2002). This diversity of amorphous systems often causes variations in pharmaceutical performance, and, in many cases, analytical methods cannot identify the structural differences. The difference in energy level would be observed as that of enthalpy recovery when a glassy material is heated across the glass transition temperature (Kawakami and Pikal, 2005). The DSC traces of the lyophilized formulations did not show any clear enthalpy recovery (Fig. 5), which suggests that the differences between the formulations are not those of the energy level. Unlike crystals, amorphous structures are characterized by an irregular disposition and loosely packed molecules, which allow for microheterogeneity in amorphous systems (Yu, 2001). In their dielectric studies on amorphous solids, Johari and Goldstein (1970) and Johari (1982) advanced the view that glass may have different regions: the glass transition (primary relaxation) involves cooperative motions in high-density regions ( $\alpha$ -region), whereas in secondary relaxation ( $\beta$ -relaxation) low-density regions ( $\beta$ -region) lie between high-density regions. Yu (2001) summarized the physical techniques for characterizing amorphous solids and classified TSDC as one of the few capable of detecting the microheterogeneity of amorphous systems.

It is reasonable to assume that TSDC could sensitively detect the structural differences in the lyophilized cakes because the differences in disposition are a kind of microheterogeneity of the amorphous solids. It is possible that the left peaks in the traces for both formulations (Fig. 4) were due to  $\beta$ -relaxation in low-density regions, and the right peaks were due to primary relaxation in relatively high-density regions, which might have caused a glass transition in DSC (Fig. 5). Heterogeneity in the amorphous microstructure can cause variations in the molecular orientation and relaxation kinetics, which results in a fingerprint for the particular structure. In these chemical environments, high sensitivity to electrical fields and varying relaxation dynamics are expected, thus TSDC has become one of the few tools that can be used to distinguish between amorphous microstructures.

## 4. Conclusion

This study deals with lot-to-lot variations in a lyophilized protein formulation. There seems to be an advantage in using TSDC to distinguish between amorphous components in solid pharmaceuticals, and this technique can be used to analyze synthetic pharmaceuticals as well as protein formulations. It is usually difficult to determine the physicochemical attributes that control the stability and performance of solid pharmaceuticals containing amorphous components. It is also difficult to characterize the differences among production lots because the variations

are often small and indistinct. Since variations in amorphous components between production lots often raise quality issues during pharmaceutical development, it is highly desirable to have analytical methods available to control the quality. In this study, TSDC was found to be capable of detecting slight, but critical, differences in amorphous microstructure. Future applications include formulation design as well as identification testing for establishing a permissible range to ensure product quality.

## Acknowledgements

We are grateful to Rigaku Corporation for their help with the TSDC experiments, and to Dr. K. Terada and Dr. E. Yonemochi of Toho University for their helpful advice.

## References

- Backton, G., 1995. Surface characterization: understanding sources of variability in the production and use of pharmaceuticals. *J. Pharm. Pharmacol.* 47, 265–275.
- Carpenter, J.F., Pikal, M.J., Chang, B.S., Randolph, T.W., 1997. Rational design of stable lyophilized protein formulations. *Pharm. Res.* 14, 969–975.
- Cline, D., Dalby, R., 2002. Predicting the quality of powders for inhalation from surface energy and area. *Pharm. Res.* 19, 1274–1277.
- Djordjevic, N.M., Rohr, G., Hinterleitner, M., Schreiber, B., 1992. Adsorption of water on cyclosporin A, from zero to finite surface coverage. *Int. J. Pharm.* 81, 21–29.
- Drago, R.S., Vogel, G.C., Needham, T.E., 1971. A four parameter equation for predicting enthalpies of adduct formation. *J. Am. Chem. Soc.* 93, 6014–6062.
- Drebushchak, V.A., Boldyreva, E.V., Drebushchak, T.N., Shutova, E.S., 2002. Synthesis and calorimetric investigation of unstable  $\beta$ -glycine. *J. Cryst. Growth* 241, 266–268.
- Feeley, J.C., York, P., Sumbly, B.S., Dicks, H., 1998. Determination of surface properties and flow characteristics of salbutamol sulphate, before and after micronisation. *Int. J. Pharm.* 172, 89–96.
- Gomez, G., Pikal, M.J., Rodriguez-Hornedo, N., 2001. Effect of initial buffer composition on pH changes during far-from-equilibrium freezing of sodium phosphate buffer solutions. *Pharm. Res.* 18, 90–97.
- Grimsey, I.M., Feeley, J.C., York, P., 2002. Analysis of the surface energy of pharmaceutical powders by inverse gas chromatography. *J. Pharm. Sci.* 91, 571–583.
- Gutmann, V., 1978. *The Donor-Acceptor Approach to Molecular Interactions*. Plenum Press, New York.
- Hancock, B.C., Shalaev, E.Y., Shamblin, S.L., 2002. Polyamorphism: a pharmaceutical science perspective. *J. Pharm. Pharmacol.* 54, 1151–1152.
- Hirakura, Y., Kojima, S., Okada, A., Yokohama, S., Yokota, S., 2004. The improved dissolution and prevention of ampoule breakage attained by the introduction of pretreatment into the production process of the lyophilized formulation of recombinant human Interleukin-11 (rhIL-11). *Int. J. Pharm.* 286, 53–67.
- Ikeda, Y., Hirayama, T., Terada, K., 2005. Application of thermally stimulated current measurement to the polymorphic characterization of drug substances. *Thermochim. Acta* 431, 195–199.
- Johari, G.P., Goldstein, M., 1970. Viscous liquids and the glass transition II secondary relaxation in glasses of rigid molecules. *J. Chem. Phys.* 53, 2372–2388.
- Johari, G.P., 1982. Effect of annealing on the secondary relaxations in glasses. *J. Chem. Phys.* 77, 4619–4626.
- Kawakami, K., Pikal, M.J., 2005. Calorimetric investigation of the structural relaxation of amorphous materials: evaluating validity of the methodologies. *J. Pharm. Sci.* 94, 948–965.
- Moura Ramos, J.J., Pinto, S.S., Diogo, H.P., 2005. Molecular mobility in raffinose in the crystalline pentahydrate form and in the amorphous anhydrous form. *Pharm. Res.* 22, 1142–1148.
- Murase, N., Franks, F., 1989. Salt precipitation during the freeze-concentration of phosphate buffer solutions. *Biophys. Chem.* 34, 293–300.
- Nail, S.L., Jiang, S., Chongprasert, S., Knopp, S.A., 2002. *Fundamentals of Freeze-Drying*. In: Nail, Akers (Eds.), Development and Manufacture of Protein Pharmaceuticals. Kluwer Academic Publishers/Plenum Press, New York, pp. 281–359.
- Newell, H.E., Buckton, G., 2004. Inverse gas chromatography: investigating whether the technique preferentially probes high energy sites for mixtures of crystalline and amorphous lactose. *Pharm. Res.* 21, 1440–1444.
- Pyne, A., Chatterjee, K., Suryanarayanan, R., 2003a. Solute crystallization in mannitol-glycine systems—implications on protein stabilization in freeze-dried formulations. *J. Pharm. Sci.* 92, 2272–2283.
- Pyne, A., Chatterjee, K., Suryanarayanan, R., 2003b. Crystalline to amorphous transition of disodium hydrogen phosphate during primary drying. *Pharm. Res.* 20, 802–803.
- Randolph, T.W., 1997. Phase separation of excipients during lyophilization: effects on protein stability. *J. Pharm. Sci.* 86, 1198–1203.
- Riddle, F.L., Fowkes, F.M., 1989. Spectral shifts in acid–base chemistry. Van der Waals contributions to acceptor numbers. *J. Am. Chem. Soc.* 112, 3259–3264.
- Roberts, R.J., Rowe, R.C., York, P., 1994. The relationship between indentation hardness of organic solids and their molecular structure. *J. Mater. Sci.* 29, 2289–2296.
- Samouillan, V., Dandurand, J., Lacabanne, C., Hornebeck, W., 2002. Molecular mobility of elastin: effect of molecular architecture. *Biomacromolecules* 3, 531–537.
- Schultz, J., Lavielle, L., 1989. Interfacial properties of carbon fibre-epoxy matrix composites. In: Lloyd, Ward, Schreiber (Eds.), *Inverse Gas Chromatography Characterization of Polymers and Other Materials*. ACS Symposium Series, vol. 391. The American Chemical Society, Washington, DC, pp. 185–202.
- Shmeis, R.A., Wang, Z., Krill, S.L., 2004a. A mechanistic investigation of an amorphous pharmaceutical and its solid dispersions, part I: a comparative analysis by thermally stimulated depolarization current and differential scanning calorimetry. *Pharm. Res.* 21, 2025–2030.
- Shmeis, R.A., Wang, Z., Krill, S.L., 2004b. A mechanistic investigation of an amorphous pharmaceutical and its solid dispersions, part II: molecular mobility and activation thermodynamic parameters. *Pharm. Res.* 21, 2031–2039.
- Sunkersett, M.R., Grimsey, I.M., Doughty, S.W., Osborn, J.C., York, P., Rowe, R.C., 2001. The changes in surface energetics with relative humidity of carbamazepine and paracetamol as measured by inverse gas chromatography. *Eur. J. Pharm. Sci.* 13, 219–225.
- Surana, R., Randall, L., Pyne, A., Vemuri, N.M., 2003. Suryanarayanan R. Determination of glass transition temperature and in situ study of the plasticizing effect of water by inverse gas chromatography. *Pharm. Res.* 20, 1647–1654.
- Ticehurst, M.D., Rowe, R.C., York, P., 1994. Determination of the surface properties of two batches of salbutamol sulphate by inverse gas chromatography. *Int. J. Pharm.* 111, 241–249.
- Ticehurst, M.D., York, P., Rowe, R.C., Dwivedi, S.K., 1996. Characterisation of the surface properties of  $\alpha$ -lactose monohydrate with inverse gas chromatography, used to detect batch variation. *Int. J. Pharm.* 141, 93–96.
- Tang, X., Pikal, M.J., 2004. Design of freeze-drying processes for pharmaceuticals: practical advice. *Pharm. Res.* 21, 191–200.
- Tong, H.H., Shekunov, B.Y., York, P., Chow, A.H., 2006. Predicting the aerosol performance of dry powder inhalation formulations by interparticulate interaction analysis using inverse gas chromatography. *J. Pharm. Sci.* 95, 228–233.
- Van Turnhout, J., 1998. Thermally stimulated discharge of electrets. In: Sessler (Ed.), *Electrets*, vol. 1, third ed. Laplacian Press, Morgan Hill, CA, pp. 106–110.
- Yokoi, Y., Yonemochi, E., Terada, K., 2004. Changes in surface properties by granulation and physicochemical stability of granulated amorphous cefditoren pivoxil with additives. *Int. J. Pharm.* 280, 67–75.
- York, P., Ticehurst, M.D., Osborn, J.C., Roberts, R.J., Rowe, R.C., 1998. Characterisation of the surface energetics of milled dl-propranolol hydrochloride

- using inverse gas chromatography and molecular modelling. *Int. J. Pharm.* 174, 179–186.
- Yoshihashi, Y., Kitano, H., Yonemochi, E., Terada, K., 2000. Quantitative correlation between initial dissolution rate and heat of fusion of drug substance. *Int. J. Pharm.* 204, 1–6.
- Yu, L., 2001. Amorphous pharmaceutical solids: preparation, characterization and stabilization. *Adv. Drug Deliv. Rev.* 48, 27–42.
- Zielinski, M., Kryszewski, M., 1977. Thermal sampling technique for the thermally stimulated discharge in polymers. *Phys. Stat. Sol.* 42, 305–314.